Competing Non-covalent Interactions in Alkali Metal Ion−Acetonitrile−Water Clusters

Timothy D. Vaden and James M. Lisy*

Department of Chemistry, University of Illinois at Urbana-Champaign, Urbana, Illinois 61801

Received: January 31, 2005; In Final Form: March 8, 2005

Competitive ion−dipole, ion−water, and water−water interactions were investigated at the molecular level in $M^+(CH_3CN)_n(H_2O)_m$ cluster ions for M = Na and K. Different [*n*,*m*] combinations for two different $n + m$ cluster sizes were characterized with infrared predissociation spectroscopy in the O−H stretch region and MP2 calculations. In all cases, no differences were observed between the two alkali metal ions. The results showed that at the $n + m = 4$ cluster size, the solvent molecules interact only with the ion, and that the interaction between the ion and the large dipole moment of CH_3CN decreases the ion−water electrostatic interactions. At the $n + m = 5$ cluster size, at least two different hydrogen-bonded structures were identified. In these structures, the ion−dipole interaction weakens the ability of the ion to polarize the hydrogen bonds and thus decreases the strength of the water−water interactions in the immediate vicinity of the alkali metal ion.

Introduction

The extraction of alkali metal ions from aqueous solution is vital to countless molecular processes throughout chemistry and biology. Specialized ionophores such as crown ethers and cryptands are used in many synthetic and analytical procedures to separate and extract ions.[1−5] Numerous ion channels and other proteins in cellular membranes extract and transport Na^+ and K^+ from the surrounding aqueous medium. To be extracted in these systems the ion must be at least partially desolvated. At the molecular level, this means that the ionophore or other macromolecule must compete with and overcome the ion−water interactions and disrupt the hydrogen bond network surrounding the ion. It is therefore important to understand the competition between the different noncovalent interactions involving the ion, the ionophore or macromolecule, and the water molecules.

In many different ionophores and ion channels the important interactions with the alkali metal ions are via dipolar moieties located on the molecule (or macromolecule). For example, the crystal structures of K^+ selective ion channels such as KcsA show that ions in the pore interact with carbonyl groups from the peptide backbone.[6,7] Crown and lariat ether molecules extract ions via interactions with multiple ethereal oxygens.[8] Indeed, a general feature of most modern ionophores is the presence of moieties possessing relatively large local dipole moments (that is, larger than that of water) such as carbonyl and cyano groups in the ion-binding regions. In addition, the large dipole moments of helices in the KcsA cavity region have been implicated in stabilizing solvated K^+.[9] Thus, ion−dipole interactions are important in extracting alkali metal ions from solvated environments.

Acetonitrile (CH_3CN) has a dipole moment of 3.92 D,[10] which is relatively large compared to the dipole moment of water, 1.85 D.[10] Additionally, CH_3CN is a small and simple molecule that can bind directly to alkali metal ions in aqueous solution. Thus, CH_3CN is a good model for local dipolar moieties in ionophores and ion channels. Indeed, cyano groups are found as moieties in some synthetic ionophores,[11] and acetonitrile itself has been shown to assist in the extraction of alkali metal ions by larger ionophores.[12] Competing ion−CH_3CN and ion−water interactions have been studied in bulk solution,[13] but detailed information on the immediate environment of the ion and the hydrogen bond network is lacking.

The competition between ion−dipole and ion−water interactions can be studied at the molecular level with hydrated cluster ions in the gas phase. Small cluster ions are amenable to both informative experiments and accurate theoretical calculations, as the ion and its immediate molecular environment are isolated from bulk solution and the complicating effects of the counterion are removed. Extensive experimental and theoretical investigations have focused on small ion−water clusters, $M^+(H_2O)_n$ (M represents an alkali metal ion throughout this work), characterizing the ion−water interactions as well as the hydrogen bond network surrounding the ion.[14−24] Competing ion−molecule interactions can be investigated by studying mixed-solvent cluster ions. Castleman and co-workers,[25] and more recently Kebarle and co-workers,[26] have studied the thermodynamics of $M^+(CH_3OH)_n(H_2O)_m$ cluster ions. In our lab, we have investigated several different mixed-solvent systems, including M^+-$(Acetone)_n(CH_3OH)_m$[27] and $M^+(Benzene)_n(H_2O)_m$.[28]

One of the most useful techniques for studying hydrated cluster ions has been infrared predissociation spectroscopy in the O−H stretch region, as these vibrational modes are highly sensitive to ion−water interactions as well as hydrogen bond formation. Both experimental and theoretical studies have demonstrated that the O−H stretch modes of gas-phase H_2O shift to lower frequency for binary alkali metal ion−water complexes, and that the magnitude of the frequency shift is directly proportional to the strength of the ion−water interaction.[16,17,22] The water O−H stretch modes also shift to lower frequency upon formation of hydrogen bonds,[29,30] and these hydrogen-bonded O−H modes are often further shifted to lower frequency in the presence of alkali metal ions as the ion can polarize (and thus strengthen) the hydrogen bond.[31] For hydrogen-bonded O−H modes, the magnitude of the frequency shift is related to the strength of the hydrogen bond.[32] Thus, IR

* Author to whom correspondence should be address. E-mail: j-lisy@uiuc.edu.

10.1021/jp050534s CCC: $30.25
Published on Web 04/05/2005

spectroscopy of the O−H groups in hydrated cluster ions yields qualitative information regarding the strength of both the ion−water and the water−water interactions. Further structural and energetic information can often be obtained from ab initio calculations in combination with the spectroscopy in order to identify IR bands and understand experimental results.

In this work, competing ion−acetonitrile, ion−water, and water−water interactions are investigated in $M^+(CH_3CN)_n(H_2O)_m$ cluster ions with IR spectroscopy and ab initio calculations for M = Na and K. The systems are probed by varying the composition of the cluster ions at a constant cluster size (that is, a constant value of $n + m$). Spectroscopic and computational results for non-hydrogen-bonded species (observed at $n + m = 4$) characterize the properties of H_2O molecules as CH_3CN molecules are sequentially added to the cluster ions and demonstrate the effect of increasing the ion−dipole interaction on the ion−water interactions. Hydrogen-bonded species are similarly characterized at $n + m = 5$ and demonstrate the impact of increasing the ion−dipole interaction on the water hydrogen bonds in proximity to the ion.

Experimental Section

The cluster ions studied in this experiment were produced and analyzed in a triple-quadrupole mass spectrometer, described in detail elsewhere.[33,34] Briefly, the alkali ions are generated from a resistively heated tungsten filament coated with a paste containing an alkali halide salt. These ions are injected into a supersonic expansion of neutral CH_3CN and H_2O molecules in argon carrier gas about 30 mm downstream from a 180-μm-diameter conical nozzle. The nascent cluster ions stabilize via evaporative cooling[35−37] and are analyzed in the mass spectrometer. The first quadrupole mass-selects the cluster ion of interest, and the third quadrupole detects fragment ions that have undergone a dissociative event. In between, a 60-cm-long RF-only quadrupole serves as an ion guide, where the cluster ions interact with a tunable IR laser. When a molecule in the cluster absorbs a photon, the energy quickly spreads throughout the cluster ion resulting in vibrational predissociation. For all cluster ions in this work, the dominant fragmentation channel is the loss of one water molecule. The IR spectrum is measured by recording the percent fragmentation as a function of IR frequency. This action spectrum is reported as the infrared predissociation (IRPD) cross section by correcting for the laser fluence. The IR source is the idler component of a $LiNbO_3$ optical parametric oscillator pumped by the 1064-nm output of a custom 20-ns pulse width Nd:YAG laser (Continuum). Absolute frequency calibration (± 2 cm^{-1}) for the spectrum is obtained by simultaneously measuring the photoacoustic spectrum of water vapor. A 3-point-averaging procedure was applied to the data as noted to smooth the reported IR spectra.

An important experimental parameter in the study of cluster ions is the internal energy content. The evaporative cooling process for the cluster ions considered in this work results in internal energies corresponding to temperatures on the order of 250−350 K.[38] Kim and co-workers have shown that under these conditions the observed structures are not always the lowest energy structures, as entropic effects may play a role.[19−21]

Ab Initio Calculations

The cluster ions were also characterized with ab initio calculations. The MP2 level of theory likely provides a reasonable description of these systems, and thus structures and vibrational frequencies were calculated at the MP2/6-31+G* level for the $Na^+(CH_3CN)_n(H_2O)_m$ cluster ions using the Gaussian 03 software package.[39]

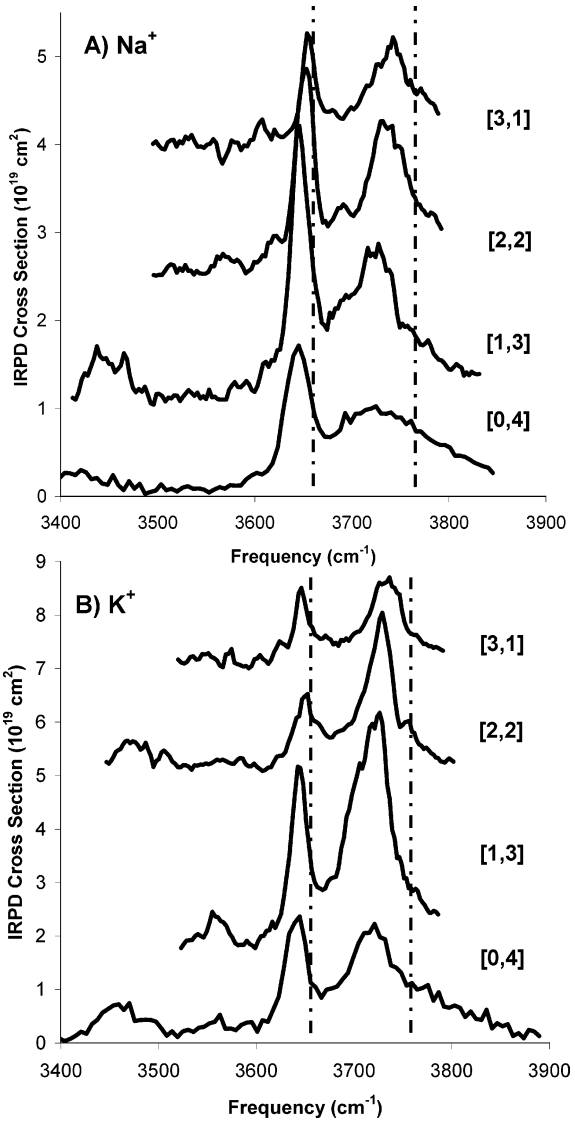

Figure 1. Smoothed IR spectra of the $M^+(CH_3CN)_n(H_2O)_m$ cluster ions for different [n,m] combinations at the $n + m = 4$ cluster size. (A) M = Na, (B) M = K. The results for the two different alkali metal ions are identical. The dotted lines in both figures show the positions of the ν_{sym} and ν_{asym} O−H stretch transitions in neutral H_2O.

Results and Discussion

$M^+(CH_3CN)_n(H_2O)_m$, $n + m = 4$. We first studied the mixed-solvent cluster ions at the nominal gas-phase solvation number of Na^+ and K^+ of four.[20,40] The effect of substituting acetonitrile molecules for water molecules is investigated by observing different [n,m] combinations. The IR spectra of $M^+(CH_3CN)_n(H_2O)_m$, M = Na and K, $n + m = 4$, are shown in Figure 1. In all spectra, two bands are observed around 3650 and 3750 cm^{-1}. These correspond to the symmetric (ν_{sym}) and asymmetric (ν_{asym}) O−H stretch modes of H_2O. The dotted lines in Figure 1 show the positions of the ν_{sym} and ν_{asym} modes in neutral H_2O at 3657 and 3756 cm^{-1}, respectively.[41] Previous work on $M^+(H_2O)_n$ cluster ions has demonstrated that the alkali metal ion−water electrostatic interaction causes a shift to lower frequency for both vibrational modes and a significant increase in the relative IR intensity of the ν_{sym} mode.[16,22] The IR spectra in Figure 1 are consistent with this as the transitions are lower

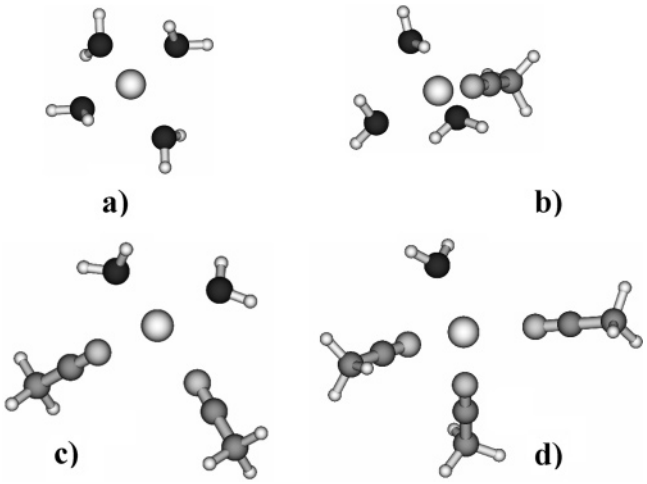

Figure 2. MP2/6-31+G* structures of the $Na^+(CH_3CN)_n(H_2O)_m$ cluster ions for $n + m = 4$. (a) [0,4], (b) [1,3], (c) [2,2], (d) [3,1].

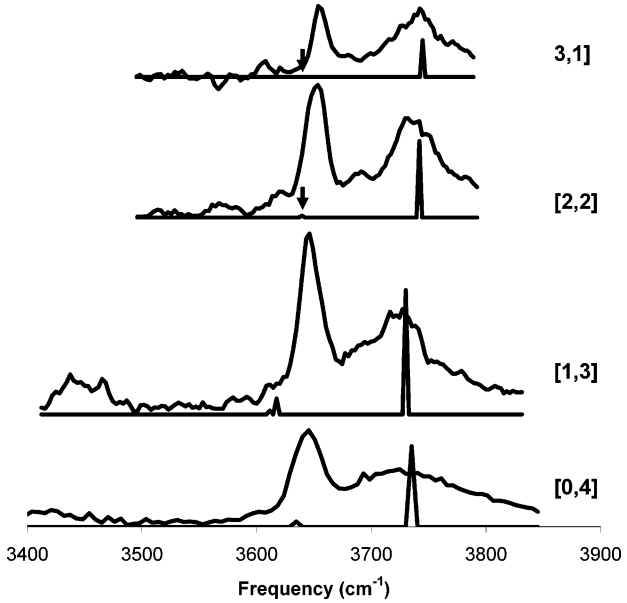

Figure 3. Vibrational frequencies (scaled by 0.97) and relative IR intensities from the computed $Na^+(CH_3CN)_n(H_2O)_m$ structures for $n + m = 4$ in Figure 2 are compared to the experimental spectra. Arrows show the positions of the ν_{sym} transition in the [2,2] and [3,1] spectra, as the predicted IR intensity of these modes is weak (see text).

than for neutral gas-phase H_2O. For the most part, the ν_{sym} and ν_{asym} transitions are the only bands observed in the spectra, indicating that no significant hydrogen bonding is present. Weak bands associated with these interactions are observed below 3600 cm^{-1} in the [0,4] and [1,3] spectra for both alkali metal ions, but can be attributed to minor isomers on the basis of intensity. Thus, at the $n + m = 4$ cluster size, the dominant interaction is between the H_2O molecules and the ion.

As CH_3CN molecules are sequentially added to the cluster ions in Figure 1, the O−H stretch transitions shift higher in frequency and gradually approach the neutral H_2O values. This immediately suggests that the ion−water interaction is progressively weakened going from the [0,4] to the [3,1] species. With Na^+, the ν_{asym} transition shifts from 3725 cm^{-1} in the [0,4] cluster ion to 3742 cm^{-1} in the [3,1] cluster ion. The change in the ν_{sym} transition is not as dramatic, but is still detectable: the frequency shifts from 3645 to 3654 cm^{-1} going from [0,4] to [3,1]. These trends are identical with those of K^+. Previous studies of non-hydrogen-bonded H_2O in mixed-solvent cluster ions in our lab, for example $M^+(Benzene)_n(H_2O)_m$[42] and Na^+-$(Difluorobenzene)_n(H_2O)_m$,[40] have not identified significant changes in the O−H stretch frequencies between different solvent combinations at the same cluster size. The difference between previous experiments and the present work is the large dipole moment of CH_3CN. Thus, Figure 1 demonstrates that the ion−dipole interaction with CH_3CN affects the strength of the ion−water interactions.

To support the spectroscopic results we calculated structures, vibrational frequencies, and binding energies at the MP2/6-31+G* level for the $Na^+(CH_3CN)_n(H_2O)_m$ cluster ions. As the K^+ spectra in Figure 1 are qualitatively identical to the Na^+ spectra, we did not perform calculations for K^+, and infer that the results of the Na^+ calculations are representative of both alkali metal ions. The structures from the MP2 calculations are shown in Figure 2. In all structures, the four solvent molecules are in the first solvent shell; that is, they are bound directly to the ion. The CH_3CN molecule binds to the Na^+ through the nitrogen atom in a linear configuration. Thus, the large dipole of the CH_3CN is completely aligned with the electric field of the alkali metal ion in these species. Cation−π interactions via the C−N triple bond were not identified in any species.

The vibrational frequencies (scaled by 0.97) and relative IR intensities from the structures in Figure 2 are compared to the experimental spectra in Figure 3. The computational results are clearly consistent with the experiments for the [0,4], [2,2], and [3,1] species. The computed O−H stretch frequencies agree quite well with the observed bands after scaling, and they increase as CH_3CN molecules are substituted for H_2O molecules. The ν_{sym} transitions are predicted to be significantly weaker than observed experimentally, but this is not unexpected on the basis of the inaccuracies in theoretical IR intensities.[43] Additionally, deriving quantitative information regarding IR intensities from action spectra can be problematic, and we thus focus our discussion on the frequencies rather than the intensities of the O−H stretch modes.

The MP2 calculations do not appear to agree as well with the [1,3] spectrum. Specifically, the O−H stretch frequencies are somewhat lower than the experimental positions and are not in line with the trend in Figure 1. The calculated [1,3] structure places all three O−O distances at 2.94 Å. In contrast, these distances in the [0,4] and [2,2] structures are around 3.7 Å. As the O−O distances in the gas-phase cyclic water trimer are 2.84 Å,[44] the calculation suggests a weak cyclic water structure, and accordingly the O−H stretch frequencies are slightly lower than would be expected in the absence of water−water interactions. However, this is not supported by the experimental spectra, which show a smooth trend from the [0,4] to the [3,1] species for both ions as presented in Figure 1. It is reasonable to assume that the structure responsible for the [1,3] IR spectrum is qualitatively identical to the [0,4], [2,2], and [3,1] species, that is, there is no hydrogen bonding. As noted in the Experimental Section, the cluster ions in our lab have an internal energy content corresponding to around 250−350 K.[38] It is reasonable to expect that, at these temperatures, the weak cyclic configuration in the computed [1,3] structure is not favored and a less-ordered structure is observed.

The effect of introducing CH_3CN to hydrated Na^+ on the ion−water interaction, as shown above, is reflected both experimentally and theoretically in the O−H vibrational frequencies. To elucidate a second example of this effect, we computed the binding energy of one H_2O molecule in the clusters for the structures in Figure 2. These binding energies (corrected for ZPE but not BSSE) are shown in Table 1. The experimental binding energy for the [0,4] cluster ion is 13.7

TABLE 1: Binding Energies (kcal/mol, corrected for ZPE) for the $Na^+(CH_3CN)_n(H_2O)_m$, $n + m = 4$, Structures

species	binding energy
[0,4]	15.7
[1,3]	14.0[a]
[2,2]	14.2
[3,1]	13.8

[a] The computed [1,3] structure is different from the experimentally observed species.

kcal/mol.[45] Thus, the MP2 calculations somewhat overestimate the ion−water interaction, which is due in part to the neglected BSSE. More important, however, is the trend in binding energies going from the [0,4] to the [3,1] species. The binding energy of H_2O clearly decreases as the CH_3CN content of the cluster ions is increased. Note that the [1,3] binding energy is somewhat out of line with the trend because this structural conformation is not observed experimentally. These binding energies are consistent with the spectroscopic results and demonstrate that the interaction between the ion and the large dipole moment of CH_3CN in the $M^+(CH_3CN)_n(H_2O)_m$ cluster ions, $n + m = 4$, effectively decreases the strength of the ion−water electrostatic interaction.

$M^+(CH_3CN)_n(H_2O)_m$, $n + m = 5$. We now proceed to the $M^+(CH_3CN)_n(H_2O)_m$ cluster ions with $n + m = 5$ and investigate the effect of sequentially substituting CH_3CN molecules for H_2O molecules by characterizing different [*n*,*m*] combinations. The IR spectra for these species with M = Na and K are shown in Figure 4. Hydrogen-bonded O−H stretch modes in hydrated cluster ions are typically observed as intense bands below 3600 cm^{-1}.[21,23,31,46] Thus, the observation of multiple intense transitions below 3600 cm^{-1} in all spectra of Figure 4 identifies the presence of multiple hydrogen-bonded configurations in these cluster ions. Transitions above 3600 cm^{-1} correspond to non-hydrogen-bonded O−H groups, which arise from ν_{sym} and ν_{asym} modes of single waters or the free O−H stretch of a water where the other O−H group is participating in a hydrogen bond.[46] These spectra show that the onset of hydrogen bonding in the $M^+(CH_3CN)_n(H_2O)_m$ cluster ions occurs at $n + m = 5$. This is consistent with several previous investigations of cluster ions with both Na^+ and K^+ in our lab, which have also identified the onset of hydrogen bonding with a total of five solvent molecules present.[42,46,47] It is also consistent with theoretical calculations that predict hydrogen-bonded cluster ions for both $Na^+(H_2O)_5$ and $K^+(H_2O)_5$.[19−21]

For both Na^+ and K^+, the IR spectra of the [0,5], [1,4], and [2,3] cluster ions are quite similar. Hydrogen-bonded O−H bands at 3460 and 3560 cm^{-1} in the Na^+ spectrum (3470 and 3570 cm^{-1} in the K^+ spectrum) indicate the presence of at least two different types of hydrogen bonds in these cluster ions. These bands likely correspond to hydrogen-bonded O−H groups in different structural isomers for a given cluster composition. As CH_3CN molecules are sequentially added to the cluster ions, the two hydrogen-bonded O−H bands gradually shift to higher frequency. The frequency shift is more dramatic with the lower-frequency band (from 3455 cm^{-1} in the [0,5] species to 3493 cm^{-1} in the [3,2] species in the Na^+ spectra), but it is also detectable with the higher-frequency band (from 3559 to 3569 cm^{-1} in the Na^+ spectra). The similarity between the spectra from the [0,5] to the [2,3] species suggests that the two hydrogen-bonded O−H bands correspond to the same types of hydrogen bond structures in all cluster ions. Indeed, the two bands are also identifiable in the [3,2] spectra, although an additional band (around 3460 cm^{-1} for both ions) is observed. The gradual shift to higher frequency of these O−H bands immediately indicates that the hydrogen bonds in the cluster ions weaken as CH_3CN molecules are added to the system.

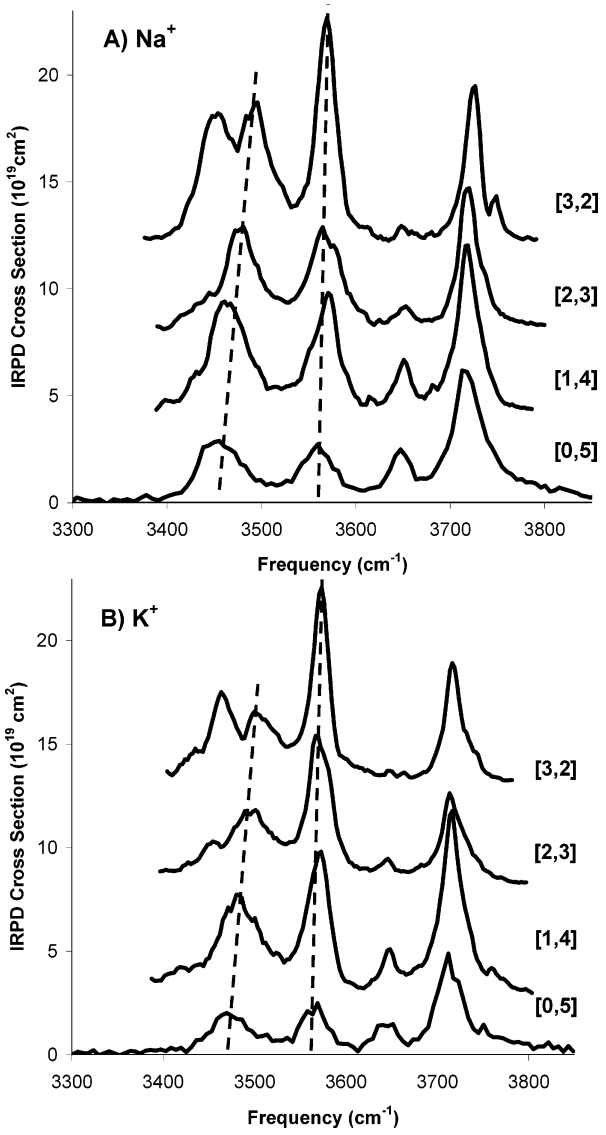

Figure 4. Smoothed IR spectra of the $M^+(CH_3CN)_n(H_2O)_m$ cluster ions for different [*n*,*m*] combinations at the $n + m = 5$ cluster size. (A) M = Na, (B) M = K. The results for the two different alkali metal ions are strikingly similar. The dotted lines illustrate that the hydrogen-bonded O−H bands below 3600 cm^{-1} shift to higher frequency as CH_3CN molecules are added.

To understand the structures corresponding to the hydrogen-bonded O−H bands in Figure 4, we computed structures and vibrational frequencies at the MP2/6-31+G* level for the $Na^+(CH_3CN)_n(H_2O)_m$, $n + m = 5$, cluster ions. As with the $n + m = 4$ species, the Na^+ and K^+ spectra are qualitatively identical and we therefore infer that the results for Na^+ are representative for both alkali metal ions. The MP2 structures are shown in Figure 5. For the [0,5], [1,4], and [2,3] species, two different structural isomers were identified, while three isomers were identified for the [3,2] species. Upon examining the structures in Figure 5, it is clear that there are two distinct types of hydrogen bond configurations in these species. In the first configuration, there is a single linear hydrogen bond between an H_2O molecule in the first solvent shell (bound to the ion) and an H_2O molecule in the second solvent shell (that is, not bound to the ion). This is the "linear" configuration and is represented by the structures on the left side of Figure 5. In the second configuration, two H_2O molecules in the first solvent

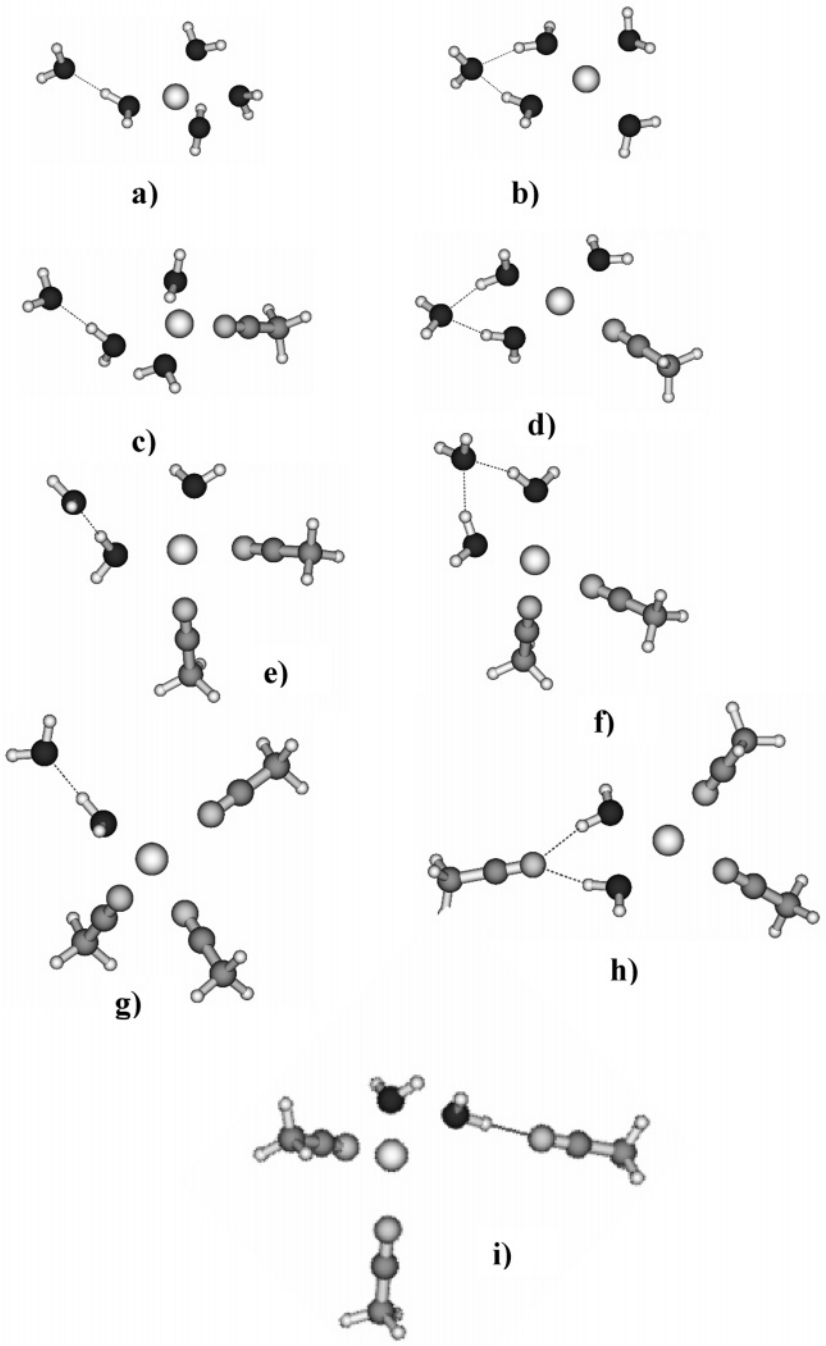

Figure 5. MP2/6-31+G* structures of the $Na^+(CH_3CN)_n(H_2O)_m$ cluster ions for $n + m = 5$. For each [*n*,*m*] combination, two different isomers ("linear" and "bent" structures, see text) are shown. (a) linear [0,5], (b) bent [0,5], (c) linear [1,4], (d) bent [1,4], (e) linear [2,3], (f) bent [2,3], (g) linear [3,2], (h) bent [3,2], (i) a third [3,2] structure.

shell are hydrogen-bonded to a single H_2O or CH_3CN molecule in the second solvent shell. This is the "bent" configuration and is represented by the structures on the right side of Figure 5. We calculated the energetic differences between the linear and bent isomers for each cluster size at 300 K (to correspond with a reasonable temperature estimate for these cluster ions) using the harmonic frequencies from the MP2 calculations. The calculations predict that for each cluster size, the bent isomer is consistently lower in energy than the linear isomer by about 3 kcal/mol. Given the fairly small energetic differences, it is quite reasonable to assume that both species will be represented in the experimental ensemble of cluster ions. A third configuration specific to the [3,2] species is represented by the structure at the bottom of Figure 5. In this structure, an H_2O molecule directly bound to the alkali metal ion forms a hydrogen bond to a CH_3CN molecule in the second solvent shell. This structure is predicted to be 1.8 kcal/mol higher in energy than the bent isomer, and it is therefore also likely present in the [3,2] cluster ion ensemble.

To compare the theoretical results to the experimental spectra, we simulated the IR spectra for the $Na^+(CH_3CN)_n(H_2O)_m$ cluster ions using the vibrational frequencies (scaled by 0.97) and relative IR intensities from the calculations. For a given [*n*,*m*] species, a theoretical spectrum for each isomer was generated using the scaled frequencies and relative intensities and Lorentzian line shapes with widths of 30 cm^{-1}. The final simulated spectra are linear combinations of the individual spectra for the different isomers, with relative populations as noted below. These theoretical spectra are presented along with the experimental spectra in Figure 6. For each cluster ion, the simulated

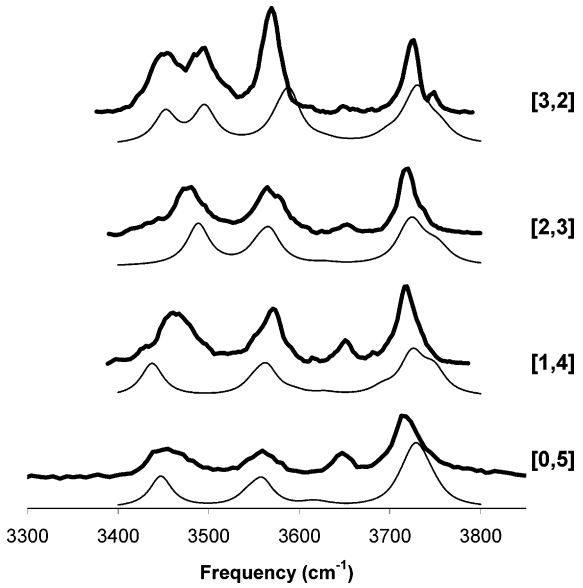

Figure 6. Simulated IR spectra for the $Na^+(CH_3CN)_n(H_2O)_m$ cluster ions, $n + m = 5$, are shown in comparison with the experimental spectra. The simulations are based on scaled frequencies and IR intensities of the bent and linear isomers from the MP2 calculations, with a Lorentzian line shape of fwhm 30 cm^{-1} for each vibrational band. For each species the simulated spectrum is the thin line (lower trace) and the experimental spectrum is the thicker line (upper trace). The simulated spectra are generated from the computed structures (refer to Figure 5) as follows: [0,5], 0.9(5a):1(5b), [1,4], 0.85(5c):1(5d), [2,3], 0.9(5e):1(5f), [3,2], 0.4(5i):0.5(5g):1(5h).

spectra show two hydrogen-bonded O−H bands, consistent with the experimental observations, with the lower-frequency band corresponding to the linear isomer and the higher-frequency band to the bent isomer. To accurately reproduce the relative intensities of the two hydrogen-bonded O−H bands, the ratios of the linear to bent isomers were 0.5:1 to 0.9:1, depending on the cluster ion. This indicates that the population of the bent isomers in these species is higher than the population of the linear isomers, which is consistent with the theoretical prediction that the bent isomers are more stable under the present conditions. For the [3,2] cluster ion, the simulated spectrum also shows a third hydrogen-bonded O−H band at 3449 cm^{-1}, which corresponds to the [3,2] isomer as shown in Figure 5i and is consistent with the experimental IR band at 3451 cm^{-1}. The ratio of this isomer to the bent isomer was 0.4:1, which is consistent with the theoretical prediction that this isomer is also less stable than the bent isomer. Note that the theoretical spectra appear to underestimate the intensity of the band around 3650 cm^{-1} (the ν_{sym} transition of non-hydrogen-bonded H_2O), as was observed with the $n + m = 4$ results.

The qualitative agreement between the MP2 calculations and the experimental results is clear from Figure 6. For the most part, the computed hydrogen-bonded O−H stretch modes gradually shift to higher frequency as CH_3CN molecules are sequentially substituted for H_2O molecules. The exception is the calculated linear hydrogen-bonded O−H band in the [1,4] spectrum, which is significantly lower than the experimental band and not in line with the trend from the [0,5] to the [3,2] spectra. The reason for this may be similar to the case of the [1,3] structure discussed above. That is, weak water−water interactions in the computed structure may be broken under the experimental conditions, and thus the observed structure is slightly different from the predicted structure due to the internal energy content of the cluster ions. Nevertheless, the results for the $Na^+(CH_3CN)_n(H_2O)_m$, $n + m = 5$, species demonstrate that the linear hydrogen bonds, and to a lesser extent the bent hydrogen bonds, are weakened by the addition of CH_3CN molecules to the cluster ions. This effect may be understood by noting the geometry of the ion−acetonitrile interaction in the computed structures (Figure 5). As with the $n + m = 4$ cluster ions, the large dipole moments of the CH_3CN molecules are completely aligned along the electric field of the alkali metal ion. The orientation of these large dipoles will decrease the electric field strength of the Na^+ and therefore reduce the ability of the ion to polarize the adjacent water molecules, with the net effect of weakening the nearby hydrogen bonds.

Taken together, the results for the $M^+(CH_3CN)_n(H_2O)_m$ cluster ions elucidate the competing ion−dipole, ion−water, and water−water interactions in the immediate molecular environment of Na^+ and K^+. In these systems, the CH_3CN molecules bind to the ion with their large dipole moment (3.92 D) aligned with the electric field of the ion. This ion−dipole interaction decreases the strength of the ion−water interactions as well as the water−water hydrogen bonds. This is an important result, as it depicts a mechanism in which local dipole moieties in ion channels and ionophores can weaken the ion−water interactions and/or disrupt the hydrogen bonding network in order to extract alkali metal ions from aqueous solution

Conclusions

The effect of ion−dipole interactions on ion−water and water−water interactions was investigated at the molecular level in mixed-solvent $M^+(CH_3CN)_n(H_2O)_m$ cluster ions for M = Na and K. Infrared predissociation spectroscopy in the O−H stretch region and MP2 calculations were used to study the effect of sequentially substituting CH_3CN molecules for H_2O molecules in these species. This was done by characterizing different [*n*,*m*] combinations of the cluster ions at a given cluster size of $n + m$.

At the $n + m = 4$ cluster size, the solvent molecules bind to the alkali metal ion in the first solvent shell. The IR spectroscopic and theoretical results demonstrate that the CH_3CN molecule interacts with the ion such that the large dipole moment of the acetonitrile is completely aligned with the electric field of the ion. The effect of this ion−dipole interaction is to weaken the ion−water electrostatic interactions. At the $n + m = 5$ cluster size, the results identify the presence of at least two different hydrogen-bonded configurations. These are represented by the linear and bent hydrogen-bonded isomers. In these cluster ions, the dipole moments of the CH_3CN molecules again are aligned with the electric field of the alkali metal ion. The dependence of the hydrogen-bonded O−H stretch transitions on the number of CH_3CN molecules present illustrates that the ion−dipole interaction weakens the hydrogen bonds in these configurations, likely by decreasing the electric field strength of the ion. These results demonstrate that interactions between alkali metal ions and local dipoles can decrease both the ion−water interactions and the water−water hydrogen bonding interactions in the immediate molecular environment of the ion.

Acknowledgment. This material is based on work supported by the National Science Foundation under Grant Nos. CHE-0415859 and CHE-0072178, and in part by a fellowship from Merck Research Laboratories. Any opinions, findings and conclusions or recommendations expressed in this material are those of the authors and do not necessarily reflect the views of the National Science Foundation. The authors would also like to thank Ms. Dorothy Miller for experimental and computational assistance.

References and Notes

(1) Ball, J. C.; Allen, J. R.; Ryu, J.-Y.; Vickery, S.; Cullen, L.; Bukowski, P.; Cynkowski, T.; Daunert, S.; Bachas, L. G. *Electroanalysis* **2002**, *14*, 186.

(2) Gokel, G. W. *Chem. Commun.* **2000**, *1*, 1.

(3) Gokel, G. W.; Mukhopadhyay, A. *Chem. Soc. Rev.* **2001**, *30*, 274.

(4) Hayashita, T.; Teramae, N.; Kuboyama, T.; Nakamura, S.; Yamamoto, H.; Nakamura, H. *J. Inclusion Phenom. Mol. Recognit. Chem.* **1998**, *32*, 251.

(5) Webber, P. R. A.; Beer, P. D.; Chen, G. Z.; Felix, V.; Drew, M. G. B. *J. Am. Chem. Soc.* **2004**, *125*, 5774.

(6) Mackinnon, R. *FEBS Lett.* **2003**, *555*, 62.

(7) Mackinnon, R. *Biosci. Rep.* **2004**, *24*, 75.

(8) Gokel, G. W.; Leevy, W. M.; Weber, M. E. *Chem. Rev.* **2004**, *104*, 2723.

(9) Roux, B.; Mackinnon, R. *Science* **1999**, *285*, 100.

(10) Lide, D. R. *CRC Handbook of Chemistry and Physics*, 78th ed.; CRC Press: New York, 1997.

(11) Paek, K.; Knobler, C. B.; Maverick, E. F.; Cram, D. J. *J. Am. Chem. Soc.* **1989**, *111*, 8662.

(12) Danil de Namor, A. F.; Pugliese, M. A.; Casal, A. R.; Aparicio-Aragon, W. B.; Piro, O. E.; Castellano, E. E. *Phys. Chem. Chem. Phys.* **2004**, *6*, 3286.

(13) O'Brien, J. F.; Johnson, D. W.; Kuehner, K.; Brewer, T. R.; Keil, R. G. *Inorg. Chim. Acta* **1991**, *183*, 113.

(14) Bauschlicher, C. W., Jr.; Langhoff, S. R.; Partridge, H.; Rice, J. E.; Komornicki, A. *J. Chem. Phys.* **1991**, *95*, 5142.

(15) Dalleska, N. F.; Tjelta, B. L.; Armentrout, P. B. *J. Phys. Chem.* **1994**, *98*, 4191.

(16) Feller, D.; Glendening, E. D.; Woon, D. E.; Feyereisen, M. W. *J. Chem. Phys.* **1995**, *103*, 3526.

(17) Glendening, E. D.; Feller, D. *J. Phys. Chem.* **1995**, *99*, 3060.

(18) Hartke, B.; Charvat, A.; Reich, M.; Abel, B. *J. Chem. Phys.* **2002**, *116*, 3588.

(19) Kim, J.; Lee, S.; Cho, S. J.; Mhin, B. J.; Kim, K. S. *J. Chem. Phys.* **1995**, *102*, 839.

(20) Lee, H. M.; Kim, J.; Lee, S.; Mhin, B. J.; Kim, K. S. *J. Chem. Phys.* **1999**, *111*, 3995.

(21) Lee, H. M.; Tarakeshwar, P.; Park, J.; Kolaski, M. R.; Yoon, Y. J.; Yi, H.-B.; Kim, W. Y.; Kim, K. S. *J. Phys. Chem. A* **2004**, *108*, 2949.

(22) Vaden, T. D.; Lisy, J. M. *J. Chem. Phys.* **2004**, *121*, 3102.

(23) Schulz, F.; Hartke, B. *Phys. Chem. Chem. Phys.* **2003**, *5*, 5021.

(24) Weinheimer, C. J.; Lisy, J. M. *J. Chem. Phys.* **1996**, *105*, 2938.

(25) Evans, D. H.; Keesee, R. G.; Castleman, A. W. *J. Phys. Chem.* **1991**, *95*, 3558.

(26) Nielsen, S. B.; Masella, M.; Kebarle, P. *J. Phys. Chem. A* **1999**, *103*, 9891.

(27) Selegue, T. J.; Cabarcos, O. M.; Lisy, J. M. *J. Chem. Phys.* **1994**, *100*, 4790.

(28) Weinheimer, C. J.; Lisy, J. M. *Chem. Phys.* **1998**, *239*, 357.

(29) Huisken, F.; Kaloudis, M.; Kulcke, A. *J. Chem. Phys.* **1996**, *104*, 17.

(30) Xantheas, S. S.; Dunning, T. H., Jr. *J. Chem. Phys.* **1993**, *99*, 8774.

(31) Lisy, J. M. *Int. Rev. Phys. Chem.* **1997**, *16*, 267.

(32) Iwakaki, A.; Fujii, A.; Watanabe, T.; Ebata, T.; Mikami, N. *J. Phys. Chem.* **1996**, *100*, 16053.

(33) Draves, J. A.; Luthey-Schulten, Z.; Liu, W.-L.; Lisy, J. M. *J. Chem. Phys.* **1990**, *93*, 4589.

(34) Weinheimer, C. J.; Lisy, J. M. *J. Phys. Chem.* **1996**, *100*, 15305.

(35) Klots, C. E. *J. Chem. Phys.* **1985**, *83*, 5854.

(36) Klots, C. E. *Z. Phys. D: At., Mol. Clusters* **1987**, *5*, 83.

(37) Klots, C. E. *J. Phys. Chem.* **1988**, *92*, 5864.

(38) Cabarcos, O. M.; Weinheimer, C. J.; Lisy, J. M. *J. Phys. Chem. A* **1999**, *103*, 8777.

(39) Frisch, M. J.; Trucks, G. W.; Schlegel, H. B.; Scuseria, G. E.; Robb, M. A.; Cheeseman, J. R.; Montgomery, J. A., Jr.; Vreven, T.; Kudin, K. N.; Burant, J. C.; Millam, J. M.; Iyengar, S. S.; Tomasi, J.; Barone, V.; Mennucci, B.; Cossi, M.; Scalmani, G.; Rega, N.; Petersson, G. A.; Nakatsuji, H.; Hada, M.; Ehara, M.; Toyota, K.; Fukuda, R.; Hasegawa, J.; Ishida, M.; Nakajima, T.; Honda, Y.; Kitao, O.; Nakai, H.; Klene, M.; Li, X.; Knox, J. E.; Hratchian, H. P.; Cross, J. B.; Adamo, C.; Jaramillo, J.; Gomperts, R.; Stratmann, R. E.; Yazyev, O.; Austin, A. J.; Cammi, R.; Pomelli, C.; Ochterski, J. W.; Ayala, P. Y.; Morokuma, K.; Voth, G. A.; Salvador, P.; Dannenberg, J. J.; Zakrzewski, V. G.; Dapprich, S.; Daniels, A. D.; Strain, M. C.; Farkas, O.; Malick, D. K.; Rabuck, A. D.; Raghavachari, K.; Foresman, J. B.; Ortiz, J. V.; Cui, Q.; Baboul, A. G.; Clifford, S.; Cioslowski, J.; Stefanov, B. B.; Liu, G.; Liashenko, A.; Piskorz, P.; Komaromi, I.; Martin, R. L.; Fox, D. J.; Keith, T.; Al-Laham, M. A.; Peng, C. Y.; Nanayakkara, A.; Challacombe, M.; Gill, P. M. W.; Johnson, B.; Chen, W.; Wong, M. W.; Gonzalez, C.; Pople, J. A. *Gaussian 03*, revision B.04; Gaussian, Inc: Pittsburgh, PA, 2003.

(40) Patwari, G. N.; Lisy, J. M. *J. Chem. Phys.* **2003**, *118*, 8555.

(41) Herzberg, G. *Molecular Spectra and Molecular Structure II. Infrared and Raman Spectra*; Van Nostrand Reinhold Company: New York, 1945.

(42) Cabarcos, O. M.; Weinheimer, C. J.; Lisy, J. M. *J. Chem. Phys.* **1999**, *110*, 8429.

(43) Galabov, B.; Yamaguchi, Y.; Remington, R. B.; Schaefer, H. F. I. *J. Phys. Chem. A* **2002**, *106*, 819.

(44) Liu, K.; Brown, M. G.; Viant, M. R.; Cruzan, J. D.; Saykally, R. J. *Mol. Phys.* **1996**, *89*, 1373.

(45) Keesee, R. G.; Castleman, A. W., Jr. *J. Phys. Chem. Ref. Data* **1986**, *15*, 1011.

(46) Vaden, T. D.; Lisy, J. M. *J. Chem. Phys.* **2004**, *120*, 721.

(47) Cabarcos, O. M.; Weinheimer, C. J.; Lisy, J. M. *J. Chem. Phys.* **1998**, *108*, 5151.